Electrochemical Investigation of the Role of Cl^- on Localized Carbon Dioxide Corrosion Behavior of Mild Steel

X. Jiang,‡, S. Nešić,** B. Kinsella,** B. Brown,** and D. Young***

ABSTRACT

Electrochemical behavior of localized carbon dioxide (CO_2) corrosion of X65 mild steel at 80°C in 0.1, 1.0, 10, and 20 wt% sodium chloride (NaCl) solutions have been investigated using electrochemical techniques including linear polarization resistance (LPR) and electrochemical impedance spectroscopy (EIS). Surface morphology of specimens was observed using scanning electron microscopy (SEM). Pit depth and its corresponding 3D optical measurement were undertaken using infinite focus microscopy (IFM). The results showed that Cl^- concentration had only a slight effect on general corrosion rate. It also revealed that increasing Cl^- concentration did not accelerate the initiation of localized corrosion; localized corrosion rate did not change with increasing NaCl solution concentrations; and chemical dissolution of corrosion product film could initiate localized CO_2 corrosion.

KEY WORDS: chemical dissolution, electrochemical techniques, initiation, localized CO_2 corrosion, mild steel, NaCl concentration

Submitted for publication: December 16, 2011. Revised and accepted: March 26, 2012. Preprint available online: July 11, 2012, http://dx.doi.org/10.5006/0620.

‡ Corresponding author. E-mail: jiangx.qday@sinopec.com.

* Institute for Corrosion and Multiphase Technology, Department of Chemical and Biomolecular Engineering, Ohio University, Athens, OH 45701. Present address: Sinopec Research Institute of Safety Engineering, No. 218, Yan'an 3rd RD, Qingdao, Shandong, 266071, P.R. China.

** Institute for Corrosion and Multiphase Technology, Department of Chemical and Biomolecular Engineering, Ohio University, Athens, OH 45701.

INTRODUCTION

In the production of petroleum, mild steel is the most frequently used material for construction of long oil and gas transmission pipelines because of its relative low cost. The production of petroleum is usually associated with production of carbon dioxide (CO_2) gas and water. When CO_2 dissolves in water, carbonic acid (H_2CO_3) is usually formed, which is more corrosive to mild steel than hydrochloric acid (HCl) at the same pH.

During the CO_2 corrosion processes, a corrosion product scale/film, mostly iron carbonate ($FeCO_3$), may precipitate on the surface of the steel, which is known to play an important role in the mechanism, kinetics, and pattern of CO_2 corrosion.[1] Any damage to the corrosion product film, for example, by mechanical removal, chemical dissolution, or the combination of both, is typically followed by severe corrosion attack.[2] Depending on the existing conditions, CO_2 corrosion of mild steel may cause either general corrosion or localized corrosion. In spite of extensive research work done in this area, failure from CO_2 corrosion still occurs. This failure is almost always a result of localized pitting corrosion. Localized corrosion commonly has been considered as developing in three stages, namely, initiation, propagation, and repassivation. It is difficult to stop localized corrosion once it begins. The mechanism of propagation of localized corrosion is reasonably well understood,[3]

ISSN 0010-9312 (print), 1938-159X (online)
13/000005/$5.00+$0.50/0

TABLE 1
Chemical Composition of X65 Mild Steel

	C	Mn	Si	P	S	Cr	Cu	Ni	Mo	Al
X65	0.065	1.54	0.25	0.013	0.001	0.05	0.04	0.04	0.007	0.041

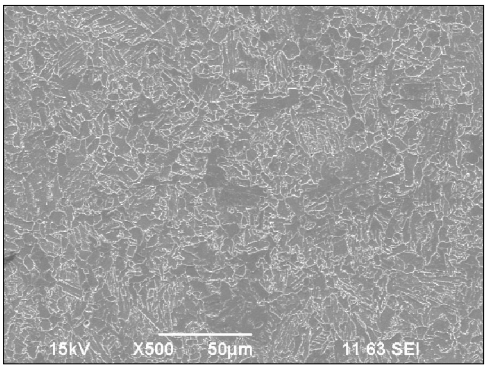

FIGURE 1. *Ferritic-pearlitic microstructure of X65 steel.*

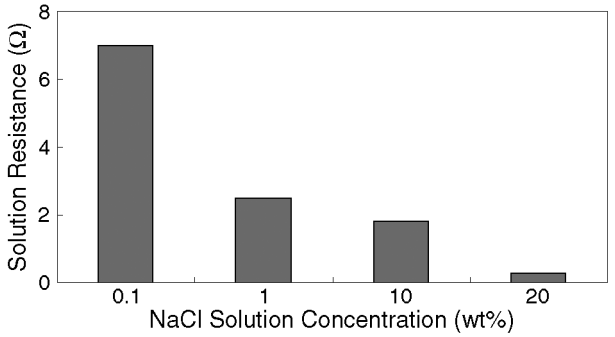

FIGURE 2. *Variation of solution resistance with NaCl concentrations (initially pH 6).*

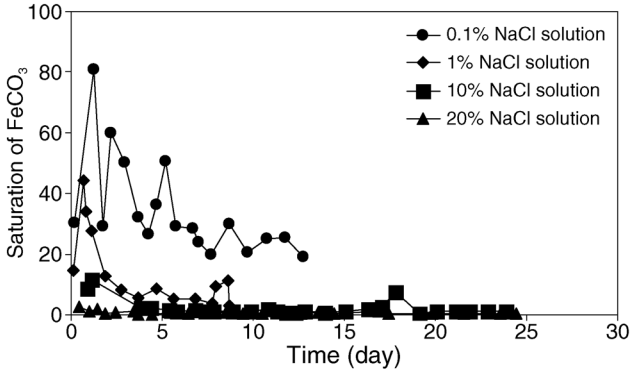

FIGURE 3. *Variation of saturation of $FeCO_3$ with time at different NaCl solutions (initially pH 6).*

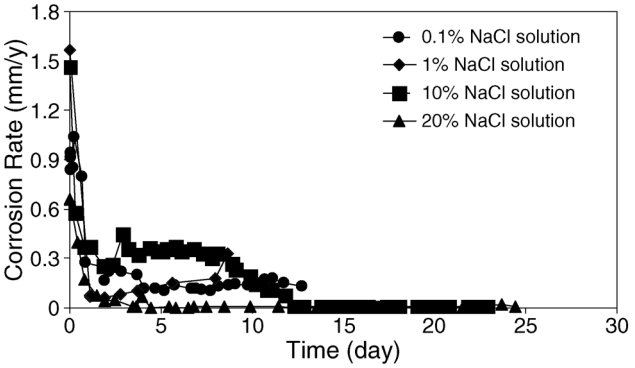

FIGURE 4. *Corrosion rate with time at different NaCl solutions (initially pH 6).*

while the mechanism of the initiation process remains unclear.

Most work about CO_2 corrosion has been done at low salt concentrations, typically from 1 wt% to 3 wt% NaCl concentrations because of the suspicion that localized corrosion may be accelerated by chloride ions at these low salt concentrations.[4-5] No significant effects of salt concentration on general CO_2 corrosion were observed at low salt concentration. Much higher salt concentrations are often present in the formation water of oil and gas reservoirs. Considerably less work has been carried out at high salt concentrations,[6-7] despite the fact that Cl^- is widely thought to be an aggressive pitting agent in aqueous solution.[8] Fang[6] investigated the influence of chloride ions under non-scaling conditions at pH 4 and up to 20% sodium chloride (NaCl) concentrations. No pitting corrosion was observed under the non-scaling conditions. The rate of uniform corrosion decreased with increasing concentrations of NaCl and this was attributed to a decrease in the solubility of CO_2 at the higher salt concentration. An important gap missing is the influence of chloride ion concentration on localized CO_2 corrosion, especially when present at high concentration, e.g., 20% NaCl.

In this paper, the role of Cl^- in the initiation stage was investigated at the range between 0.1 wt% to 20 wt% NaCl concentration. Chemical dissolution of the corrosion product film then was carried out to illustrate the initiation of localized corrosion and the role of Cl^- in the subsequent process.

EXPERIMENTAL PROCEDURES

The glass cell was filled up with 2 L of electrolyte, which consisted of distilled water and 0.1, 1.0, 10, and 20 wt% NaCl concentration, respectively. The glass cell setup is presented in another paper.[9]

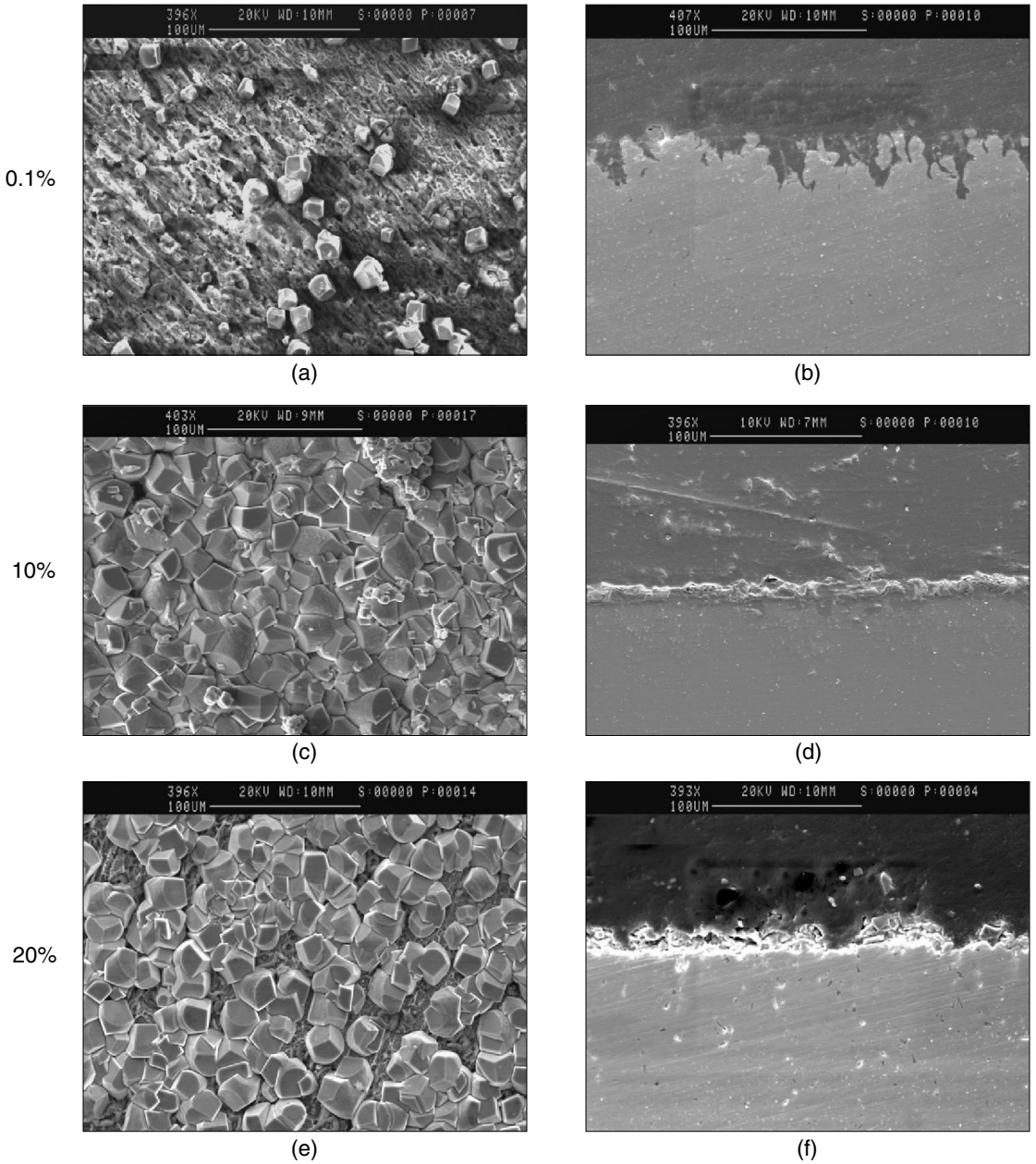

FIGURE 5. *Surface SEM images in left column and cross-sectional morphology in right column for the 0.1% NaCl solution in 1st row, 10% NaCl solution in 2nd row, and 20% NaCl solution in 3rd row, after 13 days (initially pH 6).*

All measurements were carried out at a temperature of 80°C ± 1°C with the temperature controlled by hot plate and thermocouple immersed in the solution. Prior to the experiment, the solution was deaerated by bubbling CO_2 gas for 1 h, then this was continued throughout the experiment. The total pressure in the glass cell was 1 bar. The pH was monitored with an electrode immersed in the electrolyte. Fe^{2+} concentration was measured twice daily using a spectrophotometric method. A pump was used to circulate electrolyte between the Na-based ion exchange resin and the glass cell. When required (saturation of $FeCO_3$ was lower than 0.5 or higher than 2), the pump was used to move the solution through a Na-based ion exchange resin to consume generated ferrous ion and prevent uncontrolled buildup of corrosion products in long-term experiments.

Five rectangular coupons (2.0 by 0.9 by 0.4 in) and a cylindrical coupon of X65 mild steel specimens, with the chemical composition given in Table 1 and ferritic-pearlitic microstructure shown in Figure 1, were inserted into the same glass cell in each experiment. Prior to immersion, specimens were polished with 240, 400, and 600 grit silicon carbide (SiC) paper and then rinsed with isopropanol (C_3H_8O). Two rectangular coupons were used for electrochemical noise

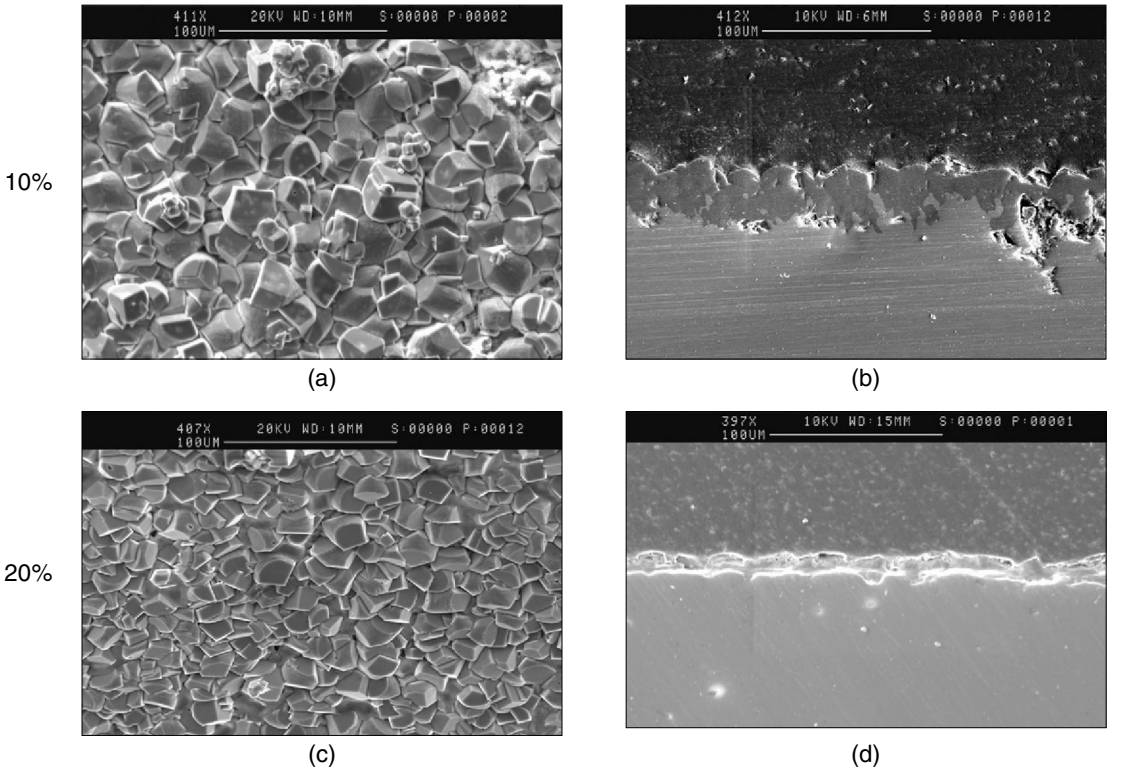

FIGURE 6. *Surface SEM images in left column and cross-sectional morphology in right column for the 10% NaCl solution in 1st row and 20% NaCl solution in 2nd row, after 27 days (initially pH 6).*

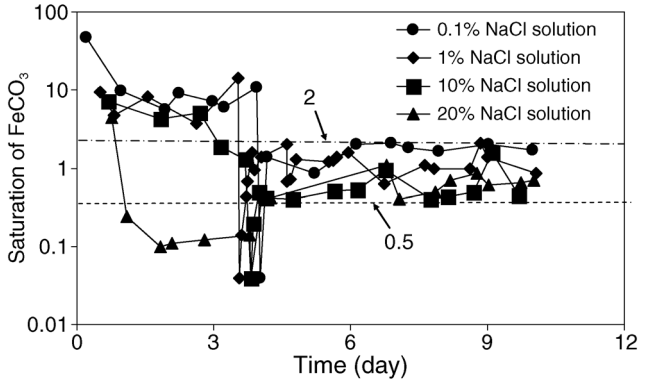

FIGURE 7. *Variation of saturation of $FeCO_3$ with time at different NaCl solutions.*

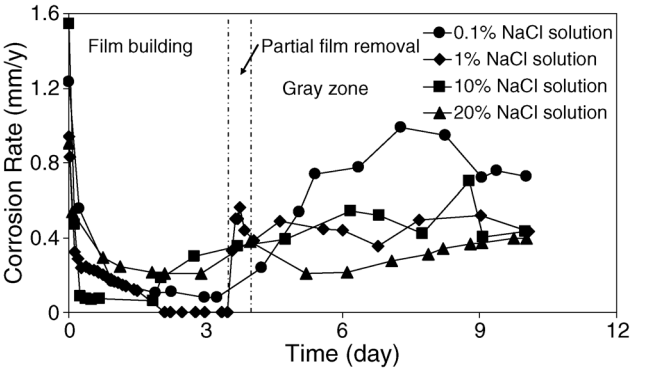

FIGURE 8. *Variation of corrosion rate with time at different NaCl solutions.*

(EN) measurement, and the results were published elsewhere;[9] three other rectangular coupons were used for scanning electron microscopy (SEM) and infinite focus microscopy (IFM) for 3D optical analysis. The cylindrical coupon with a surface area of 5.4 cm^2 was used as the working electrode (WE) for linear polarization resistance (LPR) measurements.

A standard three-electrode system incorporating a silver/silver chloride (Ag/AgCl, 3 M potassium chloride [KCl]) reference electrode and a platinum mesh counter electrode was used to obtain information of the general corrosion rate from LPR measurements. The LPR measurement was carried out by polarizing the working electrode ±5 mV vs. the open-circuit potential at a rate of 0.125 mV/s. The solution resistance was measured using electrochemical impedance spectroscopy (EIS) at an applied potential of ±5 mV vs. the corrosion potential in the frequency range from 10 kHz to 1 Hz. The solution resistance was subtracted from the polarization resistance (R_p) obtained from the LPR measurements. After the specimens were removed from the cell, they were rinsed and dried immediately, and then stored in a desiccator. Surface and cross-sectional morphology of coupons

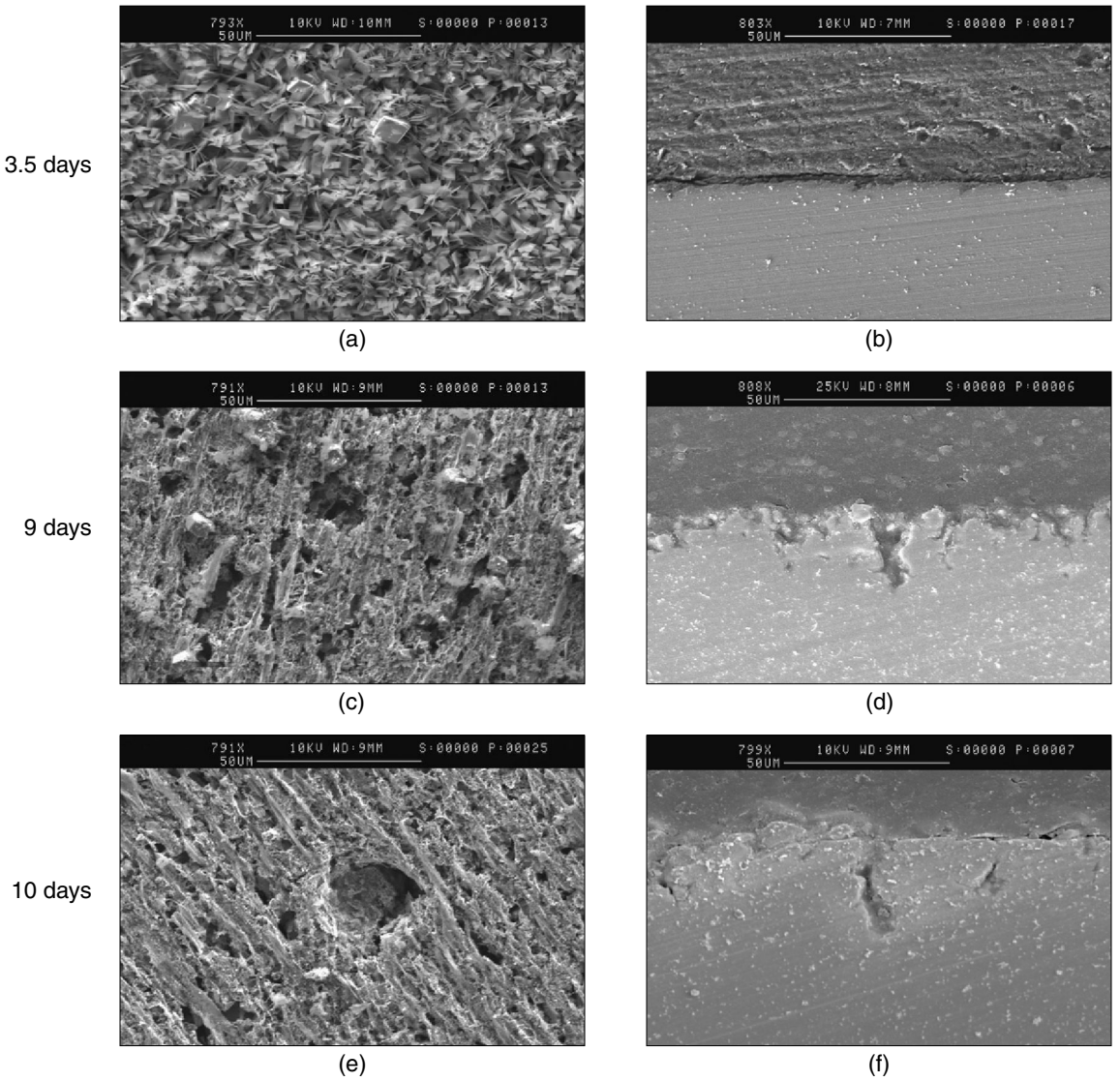

FIGURE 9. *Surface SEM images in left column and cross-section morphology in right column after 3.5 days in 1st row, 9 days in 2nd row, and 10 days in 3rd row, in 0.1% NaCl solution.*

were undertaken using SEM. The surface topography was analyzed using IFM of the surface before and after film was removed using Clarke's solution.

Two sets of experiment were conducted.

First set of experiments: The desired pH of 6.0 was obtained initially by adding sodium hydrogen carbonate ($NaHCO_3$) solution. The test duration was from 13 days to 27 days. The experimental objective was to clarify the role of Cl^- ions on the initiation of localized corrosion.

The second set of experiments had three distinct steps.

Step 1: Building of a Corrosion Product Layer — At the beginning of the experiment, the pH was adjusted to 6.3 by adding a deoxygenated $NaHCO_3$ solution. Saturation (S) of 200 with respect to $FeCO_3$ was set by injection of a deoxygenated ferrous chloride ($FeCl_2$) solution. The steel coupons were inserted and the conditions maintained for approximately 3.5 days, during which the saturation of the solution decreased as the precipitation of $FeCO_3$ occurred. This led to a significant reduction of the corrosion rate of the steel coupons.

Step 2: Partial Dissolution of the Corrosion Product Layer — Once the protective corrosion product layer was in place, the pH was adjusted to pH 5.0 and the saturation with respect to $FeCO_3$ was adjusted to 0.04. This resulted in rapid product layer dissolution. This present condition was maintained for 4 h to achieve a partial dissolution of the corrosion product layer.

Step 3: Localized Corrosion — Following the partial dissolution of the protective corrosion product layer, a pH of 6.0 was established and the saturation of $FeCO_3$ was adjusted back into the "gray zone" (S = 0.5 ~ 2.0) using a sodium-based ion exchange resin

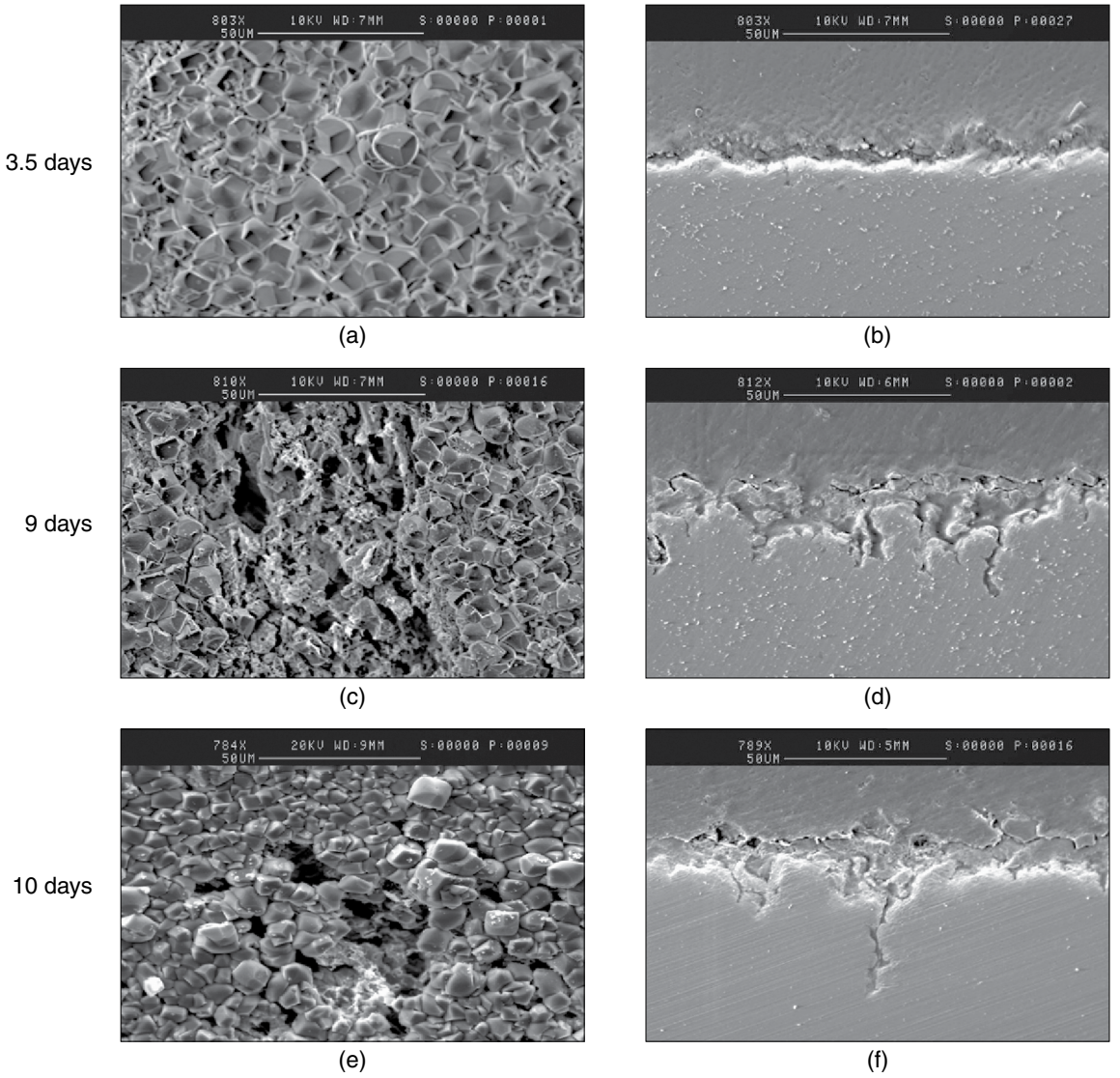

FIGURE 10. *Surface SEM images in left column and cross-sectional morphology in right column after 3.5 days in 1st row, 9 days in 2nd row, and 10 days in 3rd row, in 1% NaCl solution.*

where the corrosion product layer is certain neither to dissolve nor precipitate. Previous research indicated that "gray-zone" conditions are favorable for localized corrosion propagation.[3-4]

These conditions were maintained for approximately 6.5 days, and the total time to complete each test was about 10 days.

The second set of experiments was conducted to illustrate the initiation of localized corrosion by chemical dissolution of corrosion product film and the role of Cl^- in subsequent processes.

RESULTS AND DISCUSSION

Role of Cl^- in the Initiation of Localized Corrosion

This section discusses the results from the first set of experiments that were carried out at 80°C and an initial pH of 6.

The variation of solution resistance with NaCl concentrations at 80°C is shown in Figure 2. The solution resistance decreased with increasing NaCl concentrations as a result of the increase of ionic strength and solution conductivity.

The variation of saturation of $FeCO_3$ with time at different NaCl solutions is illustrated in Figure 3. Saturation of $FeCO_3$ was calculated according to species concentrations and the solubility constant (K_{sp}) was determined as shown in the formula below, Equation (1):

$$S = \frac{c_{Fe^{2+}} c_{CO_3^{2-}}}{K_{sp}} \quad (1)$$

All the saturations of $FeCO_3$ in Figure 3 were greater than 1. The saturation of $FeCO_3$ decreased with increasing NaCl concentrations. This means

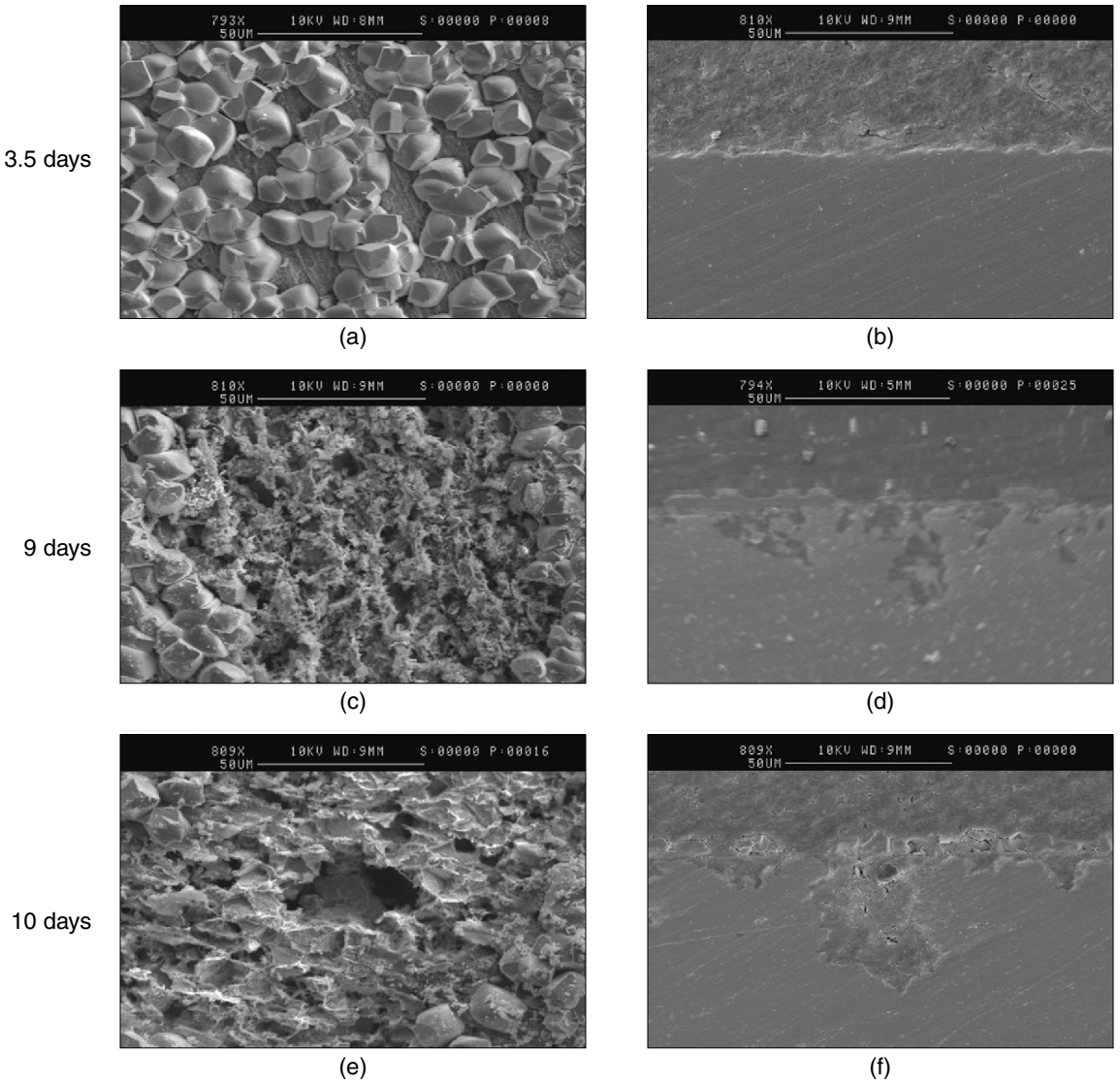

FIGURE 11. *Surface SEM images in left column and cross-sectional morphology in right column after 3.5 days in 1st row, 9 days in 2nd row, and 10 days in 3rd row, in 10% NaCl solution.*

that precipitation of $FeCO_3$ was the main process that occurred on the metal surface.

General corrosion rates measured using LPR technique with time for different NaCl solution concentrations are shown in Figure 4. The measured corrosion rates also decreased rapidly with time because of the deposition of an $FeCO_3$ corrosion product film onto the metal surface. This deposition slowed corrosion by presenting a physical barrier for the species involved in the corrosion process. No significant difference of corrosion rate was observed prior to 13 days. Localized attack in CO_2 corrosion of mild steel was always associated with the formation and breakdown of protective $FeCO_3$ films. Work performed by Cheng, et al.,[10] showed that the role of chloride ions was to increase the probability of the breakdown of the corrosion product film. If this is the case for the present system, the breakdown of corrosion product film is more likely to occur at high salt concentrations at longer immersion times. Therefore, a 27 days' immersion was carried out for 10 wt% and 20 wt% NaCl solutions. The corrosion rates were around 0.1 mm/y in both 10 wt% NaCl and 20 wt% NaCl solution when the immersion time was longer than 13 days. The result indicated that increasing Cl^- concentration had no significant effect on general corrosion rate under the conditions where protective $FeCO_3$ layers formed. This was different from Fang's work[6] where uniform corrosion rates were reported to decrease with increased NaCl concentrations, because the latter experiments were done under conditions where protective $FeCO_3$ layers are absent.

The surface and cross-sectional morphology of the steel after 13 days and 27 days at different NaCl concentrations are shown in Figures 5 and 6 to inspect localized corrosion in the present work.

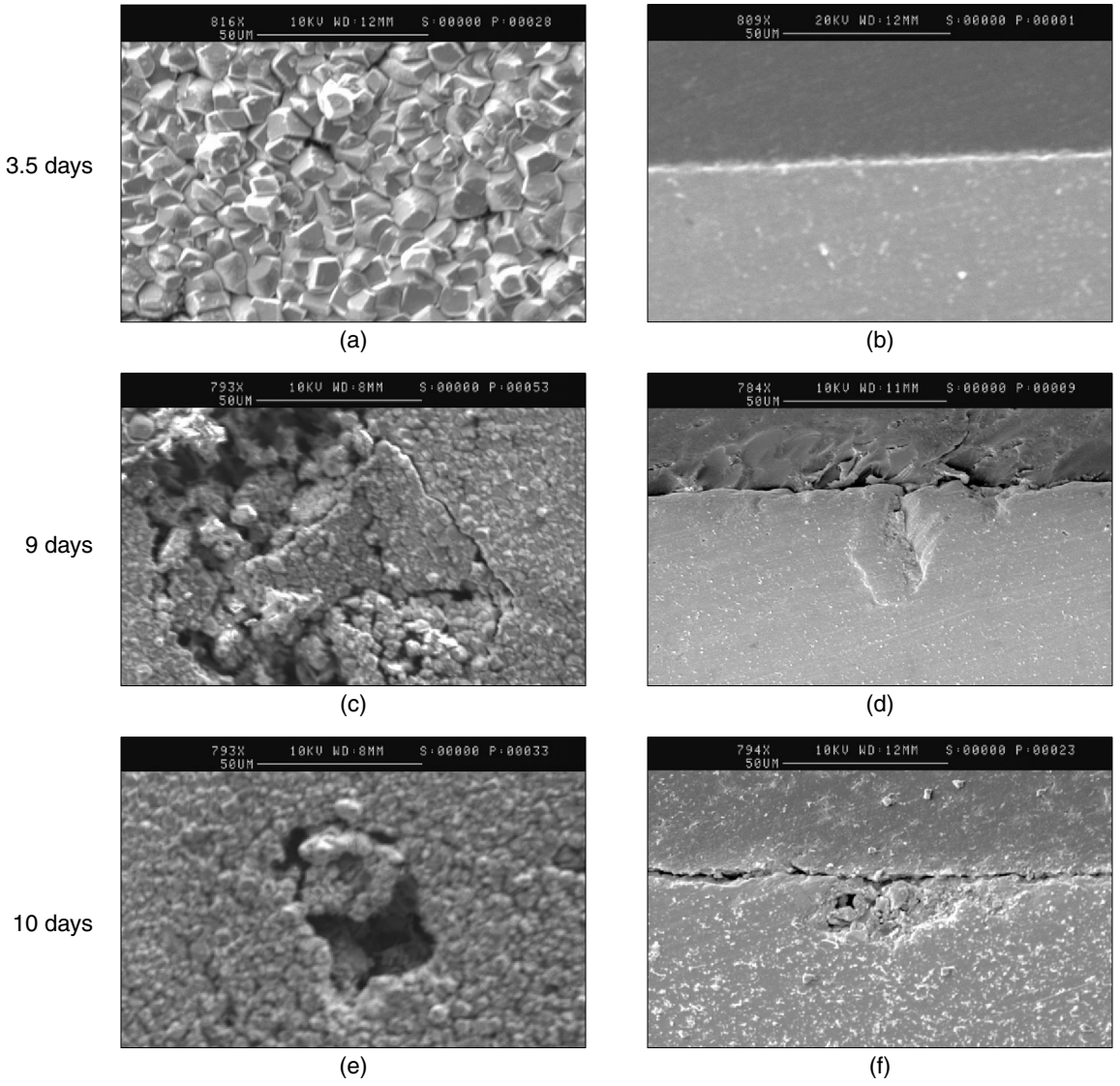

FIGURE 12. *Surface SEM images in left column and cross-sectional morphology in right column after 3.5 days in 1st row, 9 days in 2nd row, and 10 days in 3rd row, in 20% NaCl solution.*

Porous and loosely adherent film with less $FeCO_3$ particles in 0.1 wt% NaCl solution and denser corrosion product film with high crystallinity in 10 wt% and 20 wt% NaCl solutions was observed after 13 days from the surface morphology and cross-sectional SEM in Figure 5. The change of the film with the concentrations of NaCl solution may be related to the ion strength of the solution and its effect on the nucleation of $FeCO_3$ and $FeCO_3$ particle growth rate.[11] The ion strength of the solution increases with the increasing of NaCl solution. The rate of nucleation and the rate of particle growth of $FeCO_3$ may increase with the ion strength of the solution, so it was easier to obtain denser film with high crystallinity at higher concentrations of NaCl solution. Compared to the corrosion product film after 13 days, it became denser and thicker after 27 days in 10 wt% and 20 wt% NaCl solutions as shown in Figure 6, which was from the gradual deposition of corrosion product with time. No pitting or other forms of localized corrosion were evident on the steel surface after the scale was removed using inhibited HCl and inspected by SEM after both 13 days and 27 days. Despite the fact that the level of $FeCO_3$ saturation was close to unity and in the "gray zone," there was no evidence of localized attack on the scale by the high chloride ion solutions. This means that higher concentrations of chloride ions did not cause or accelerate the breakdown of the corrosion product film/scale as previously suspected. Therefore, it is concluded that chloride ion alone is not enough to initiate localized corrosion of mild steel in CO_2 environments.

Chemical Dissolution of Corrosion Product Film

If localized corrosion is not initiated by increasing Cl^- concentrations, the question that needed to be

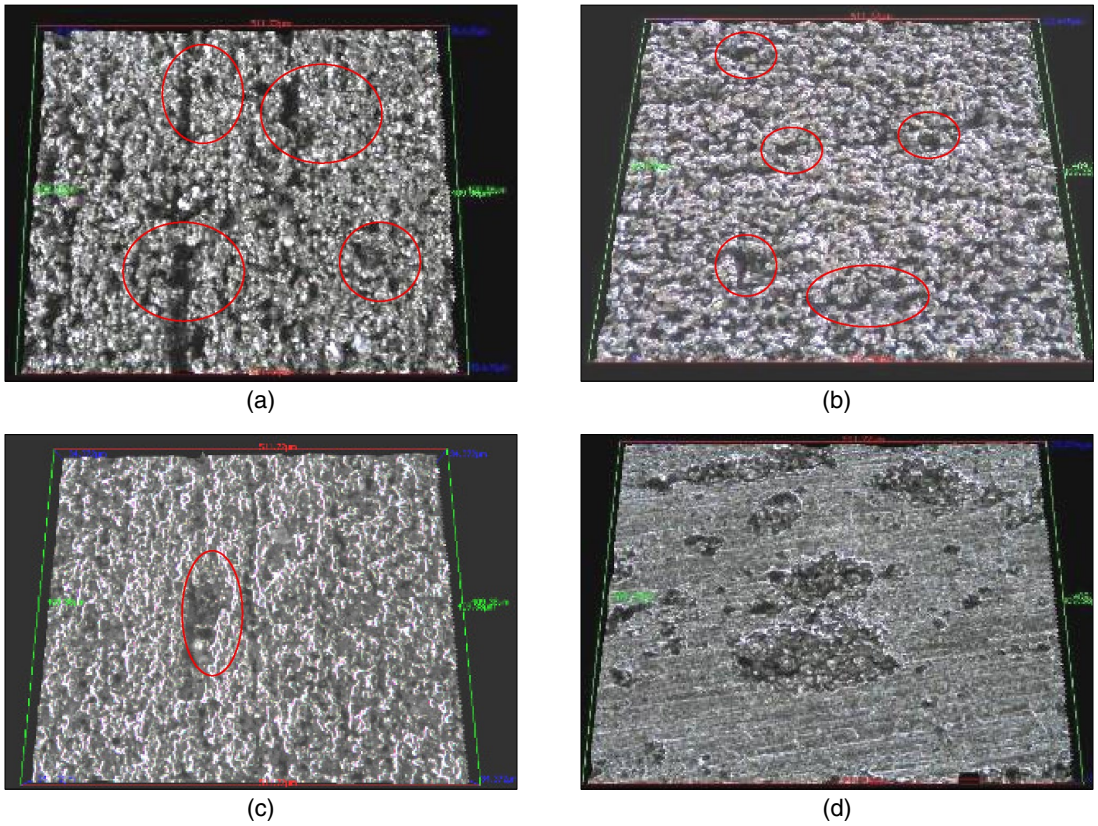

FIGURE 13. *IFM topography without corrosion product film after 10 days in (a) 0.1%, (b) 1%, (c) 10%, and (d) 20% NaCl solution.*

answered is, what influence does chloride ions have once localized corrosion is initiated. The second set of experiments was carried out in this part to clarify the initiation of localized corrosion by chemical dissolution of corrosion product film and to ascertain the role of Cl^- in subsequent processes.

The variation of saturation of $FeCO_3$ and corresponding uniform corrosion rate measured on the cylinder electrode with time in different concentrations of NaCl solutions is presented in Figures 7 and 8. The level of $FeCO_3$ saturation and corrosion rate dropped significantly over the 3.5 days in which it was observed as a result of the formation of a protective $FeCO_3$ layer. The saturation was then adjusted to 0.04, and this process was maintained for 4 h in step 2. This corresponded to a gradual increase in corrosion rate (Figure 8) since the corrosion product film was partially dissolved. The saturation was finally controlled to the "gray zone" (S = 0.5~2.0) at around 1 after 3.5 days in step 3. This meant that in the process of step 3 no more $FeCO_3$ was appreciably deposited nor was any significantly dissolved.

The surface and cross-sectional morphology in 0.1, 1.0, 10, and 20% NaCl solution after 3.5 days, 9 days, and 10 days are shown in Figures 9 through 12. Loosely adherent $FeCO_3$ film with smaller flake crystals was observed in the 0.1% NaCl solution in Figure 9, and denser $FeCO_3$ film with hexahedron crystals was obtained in Figures 10 through 12 for other NaCl solutions after 3.5 days. This also may be attributed to the effect of the ion strength on the nucleation of $FeCO_3$ and $FeCO_3$ particle growth rate. In the 0.1% NaCl solution, virtually almost all the $FeCO_3$ crystals have been removed after 9 days and 10 days. Figures 10, 11, and 12 reveal the remains of $FeCO_3$ crystals and significantly damaged $FeCO_3$ scales for 1.0, 10, and 20% NaCl solution after 9 days and 10 days from the partial dissolution that took place where the pH was reduced to 0.04 for 4 h. Localized corrosion was observed from cross-sectional morphology across the whole range of NaCl concentrations after 9 days and 10 days, and this was further confirmed in the IFM images (Figure 13) when the corrosion product layer was removed after a 10-day exposure. Therefore, one can conclude that the chemical dissolution initiated the localized CO_2 corrosion for each concentration of NaCl tested.

In the oil industry, one deep pit can cause leakage of the pipeline and even closure of the oil field. Therefore, knowledge of maximum localized corrosion rate is a very important parameter for indicating the severity of localized corrosion. In this work, maximum localized corrosion penetration rate was calculated from the maximum pit depth detected in the IFM

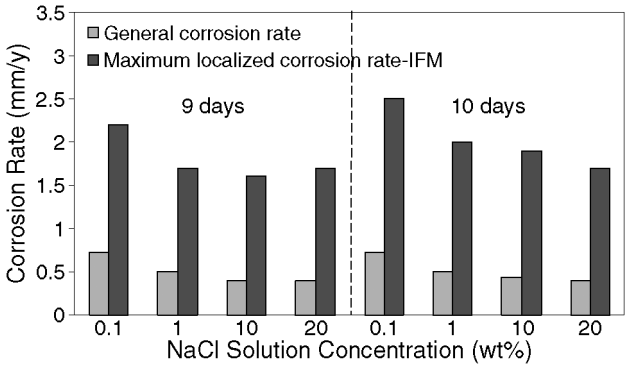

FIGURE 14. *Variation of corrosion rate with NaCl concentration after 9 days and 10 days.*

images (Figure 13). A comparison of the general corrosion rate and maximum localized corrosion rate over 9 day and 10 day exposure times for different NaCl concentrations is presented in Figure 14. There was no significant difference of general corrosion rate and maximum localized corrosion rate over the studied NaCl concentration range after 9 days and 10 days. In all cases, the final general corrosion rate is around 0.5 mm/y and the maximum time-averaged localized corrosion rate is around 2 mm/y. Neither of them changed with increasing NaCl concentrations. Therefore, NaCl concentration had very little influence on the rate of pitting corrosion once pitting corrosion was started by partial dissolution of the $FeCO_3$ scale.

CONCLUSIONS

❖ The chloride concentration had no significant effect on general CO_2 corrosion rate under conditions where protective $FeCO_3$ layers formed under static conditions.

❖ Chloride ion did not cause or accelerate the breakdown of the $FeCO_3$ layer as suspected; therefore, it was not possible to initiate localized corrosion of mild steel in CO_2 environments solely by having a high chloride concentration under static conditions.

❖ Chemical dissolution of the corrosion product initiated localized CO_2 corrosion. However, high chloride concentration had very little influence on the rate of pitting corrosion once pitting corrosion was started by partial dissolution of the $FeCO_3$ scale/film.

ACKNOWLEDGMENTS

The authors would like to acknowledge the companies who provided the financial support and technical guidance for this project. They are BP, Champion Technologies, Clariant, ConocoPhillips, Tenaris, Chevron, Baker Hughes, Baker Petrolite, PTTEP, Eni, OXY, ExxonMobil, Mi SWACO, NALCO, Saudi Aramco, Shell, Columbia Gas Transmission, and Total.

REFERENCES

1. C.A. Palacios, J.R. Shadley, *Corrosion* 47, 2 (1991): p. 122, doi: http://dx.doi.org/10.5006/1.3585227.
2. V. Ruzic, "Mechanisms of Protective $FeCO_3$ Film Remove in Single-Phase Flow-Accelerated CO_2 Corrosion of Mild Steel" (Ph.D. thesis, The University of Queensland, 2006).
3. J.B. Han, Y. Yang, B. Brown, S. Nešić, "Electrochemical Investigation of Localized Corrosion on Mild Steel," CORROSION/2007, paper no. 07323 (Houston, TX: NACE International, 2007).
4. Y.F. Sun, K. Gorge, S. Nešić, "The Effect of Cl^- and Acetic Acid on Localized CO_2 Corrosion in Wet Gas Flow," CORROSION/2003, paper no. 03327 (Houston, TX: NACE, 2003).
5. X. Jiang, Y.G. Zheng, D.R. Qu, W. Ke, *Corros. Sci.* 48, 10 (2006): p. 3091.
6. H.T. Fang, "Low Temperature and High Salt Concentration Effects on General CO_2 Corrosion for Carbon Steel" (thesis, Ohio University, 2006).
7. N. Sridhar, D.S. Dunn, A.M. Anderko, M.M. Lencka, H.U. Schutt, *Corrosion* 57, 3 (2001): p. 221, doi: http://dx.doi.org/10.5006/1.3290347.
8. M. Ergun, A.Y. Turan, *Corros. Sci.* 32, 10 (1991): p. 1137.
9. X. Jiang, S. Nešić, "Electrochemical Investigation of the Role of Cl^- on Localized Corrosion CO_2 Corrosion of Mild Steel," 17th Int. Corrosion Congress, paper no. 2414 (Houston, TX: NACE, 2008).
10. Y.F. Cheng, M. Wilmott, J.L. Luo, *Appl. Surf. Sci.* 152 (1999): p. 161.
11. A. Dugstad, "Mechanism of Protective Film Formation During CO_2 Corrosion of Carbon Steel," CORROSION/98, paper no. 031 (Houston, TX: NACE, 1998).